

1 **Authors:**

2 Corresponding author:

3 **Quinn Asena:**

- 4 • qasena@wisc.edu
- 5 • Address from which the work was done:
- 6 School of Environment, University of Auckland, 23 Symonds Street, Auckland, New Zealand
- 7 1010.
- 8 • Present address: Department of Geography, University of Wisconsin-Madison, Science Hall,
- 9 Madison, WI, 53703

10 Co-authors:

11 **George L. W. Perry:**

- 12 • george.perry@auckland.ac.nz
- 13 • School of Environment, University of Auckland, 23 Symonds Street, Auckland, New Zealand
- 14 1010.

15 **Janet M. Wilmshurst:**

- 16 • Wilmshurstj@landcareresearch.co.nz
- 17 • Manaaki Whenua – Landcare Research, 76 Gerald Street, Lincoln, New Zealand, 7608

18

19 **Keywords:** palaeoecology; paleolimnology; ecological modelling; pseudoproxy; proxy
20 system modelling; virtual ecology; uncertainty; pseudoproxy modelling;

21 Information loss in palaeoecological data from process and 22 observer error

23 Quinn Asena, George L. W. Perry, and Janet M. Wilmshurst

24 Abstract

25 Palaeoecological data provide insight into how ecosystems have changed in the past, and,
26 with the development of new sources of proxy data and statistical methods, they are being
27 used to address questions around the underlying mechanisms of change, such as biotic-
28 and climate-ecosystem interactions. However, inferences from palaeoecological data can be
29 hindered by uncertainties inherent in core-type samples that arise from environmental
30 processes and observer-introduced error. Environmental processes, core extraction
31 methods, sub-sampling strategies, laboratory methods, and data processing can potentially
32 mask 'true' signals in the data. How different sources of uncertainty influence the
33 inferences drawn from palaeoecological data is rarely assessed, but is critical to the
34 confidence of our conclusions. To address this concern, we use a virtual ecological
35 approach to assess the effects of environmental and observer introduced uncertainty to
36 better understand which of them most influence statistical methods applied to the data.
37 Quantifying information loss from uncertainty can inform study design before a project is
38 carried out, and so increase the likelihood of detecting a given signal of interest and make
39 more robust inferences from statistical analyses of palaeoproxy data. We generate
40 synthetic 'error-free' core-type samples of pseudoproxies, on which environmental and
41 observational processes are systematically introduced to impose uncertainties on the
42 simulated pseudoproxies. The influence of three sources of uncertainty (core mixing, sub-
43 sampling, and proxy quantification from sub-samples), are assessed for their individual
44 and combined effects on two statistical methods used to synthesise palaeoecological
45 records: Fisher Information and principal curves. Increasing sub-sampling intervals has the
46 most influence on the two statistical methods applied to the pseudoproxy data. When
47 combined, the interaction between increasing sub-sampling interval, and decreasing the
48 number of proxies counted per sub-sample has the strongest influence on Fisher
49 Information and principal curves. Fisher Information and principal curves are not affected
50 in the same way by introducing uncertainty, with principal curves being less influenced by
51 simulated proxy counting and sub-sampling of the core. Virtually assessing uncertainties is
52 a powerful method to better understand the influence that uncertainties introduced at
53 different parts of the analytical process have on conclusions drawn from palaeoecological
54 data.

55 1 Introduction

56 Palaeoecological data extends the temporal extent over which we can investigate
57 ecosystem change well beyond the observational record (Kosnik and Kowalewski, 2016).
58 These long-term records are crucial for understanding ecosystem trajectories and climate-
59 ecosystem interactions, as such dynamics may unfold over centuries or millennia (Jackson,
60 2007). Many proxies and statistical methods are used to address how ecosystems respond

61 to environmental and human pressures through time. Palaeoecologists use these data to go
 62 beyond describing past changes in, for example, the relative abundances of species, to
 63 uncover underlying mechanisms of change such as biotic interactions and species-
 64 environment relationships (Williams et al., 2011). However, the inferences drawn from
 65 palaeoecological data may be limited by their uncertainties, such as a paucity of
 66 observations over time and space, environmental degradation of samples, and observer-
 67 introduced error. Thus, to make robust inferences from palaeoecological data, such
 68 uncertainties need to be better understood and quantified. Here, we focus on proxies
 69 reflecting species community data such as fossil pollen extracted from a core sample and
 70 quantified on microscope slides.

71 **1.1 Uncertainties in palaeoecological data**

72 Palaeoecological data derived from core-type samples are subject to numerous
 73 uncertainties, including: (i) environmental effects and landscape processes affecting the
 74 sample before extraction; (ii) the methods used in the field to extract the sample; (iii)
 75 laboratory techniques applied to extract and quantify data from the core; and (iv)
 76 quantitative analyses applied to the data (Table 1). Environmental processes and
 77 observation error can affect the representation of species in the data (e.g., their observed
 78 relative abundances; Goring et al., 2013). Sub-sampling strategies may alter the
 79 chronological placement of events (Liu et al., 2012; Parnell et al., 2008). Manipulation of
 80 data, such as interpolation to satisfy statistical assumptions, can introduce statistical
 81 artifacts and increase type-I error rates (i.e., a false positive). Such uncertainties affect the
 82 robustness of statistical results and the inferences we may draw from them.

Table 1: Sources of uncertainty from pre-sampling natural processes to statistical analyses of data. Uncertainties are not independent across categories and can propagate through the observational process and subsequent analyses.

Source of Uncertainty	Examples
Physical, chemical and biological processes acting on the core or proxy. Not introduced by the observer.	Hiatuses, catchment erosion, variable sedimentation rates and mixing, bioturbation, changing sources of sediment or peat over time, preservation and taphonomy, occurrence of proxy in sample vs. actual abundance, differential preservation of proxies.
Observer introduced error from sampling collection and protocol.	Core compression during extraction, coring location (within basin or broader geographical context), sample depth/length and replication, core overlap, contamination.
Post-collection methods applied a sample and subsamples.	Contiguous/non-contiguous sub-sampling, sub-sampling resolution/density/thickness, sampling error/noise, proxy selection, taxonomic resolution, count method and proxy specific method error,

Data processing and interpretation.

dating frequency, dating precision and accuracy, observational error in proxy count.

Age-depth modelling, radiocarbon calibration, detrending, time-averaging, statistical methods selection, and understanding of proxy responses to environmental drivers.

83 1.2 Pseudoproxy experiments and virtual ecology

84 Virtual ecology (VE) can be used to assess the influence of uncertainty on statistical
85 methods and associated inferences (Zurell et al., 2010). In the VE approach, simulated data
86 are used as testbeds for recreating, in simulation, observational processes. The synthetic
87 data provide an ‘error-free’ benchmark against which to assess simulated observational
88 processes and analytical methods. The underlying concept is that the synthetic data mimic
89 the statistical properties of empirical data without being subject to the same issues of, for
90 example, limited grain size or extent (Smerdon, 2012). Similarly, the simulated
91 observational process aims to recreate the statistical properties of the observer, such as the
92 chance of observing a species occurring at low abundances. Here, we adopt a VE approach
93 to (i) assess uncertainties introduced by environmental processes and observer-introduced
94 error by simulating data analogous to a sediment core-type sample, and (ii) to virtually
95 recreate environmental processes acting on a core, and the observational methods used to
96 extract data from the core sample. The VE approach follows the form: generate data →
97 simulate the observational process → analyse the ‘true’ and ‘observed’ data → assess the
98 analyses of the observed data against the ‘true’ data. We extend this approach to include
99 simulated environmental process errors that occur before the observational process. The
100 steps of our adapted VE approach: data generation, degradation, observation, analysis, and
101 assessment are described in sections 2.1 through 2.3. Empirical data typically lack an
102 ‘error-free’ control, and even high-quality empirical data (e.g., highly resolved proxy data
103 from a laminated lake sediment core) incorporate multiple uncontrollable sources of
104 uncertainty. Virtual experimentation allows for the effects of sources of uncertainty to be
105 explored for their individual and interaction effects in a systematic and controlled way
106 (Smerdon, 2012).

107 The VE approach is similar to pseudoproxy experiments where modified observational
108 data or pseudoproxies (i.e., simulated proxy data) are used in place of empirical
109 observations (Mann and Rutherford, 2002) and analysed in the same way as empirical
110 measurements (Asena et al., 2024). Pseudoproxy experiments originated in climatology
111 where they are a method of assessing palaeoclimate reconstructions (Mann and
112 Rutherford, 2002; Christiansen et al., 2009; Bothe et al., 2019); here, we apply the same
113 concepts to palaeoecological data. We use the term virtual ecology to describe the approach
114 by which synthetic data are generated, sampled from and analysed in ways comparable to
115 empirical data (Zurell et al., 2010). While simulated data cannot substitute entirely for
116 reality, they provide an experimental platform (*sensu* Peck, 2004) with which to
117 understand the processes that influence the formation and analysis of empirical data.

118 Pseudoproxies have been widely used in climatology (Mann and Rutherford, 2002; Bothe et
119 al., 2019), but virtually assessing sampling methods and statistical approaches on
120 palaeoecologically relevant data is less common (although see Asena et al., 2024; Blaauwet
121 al., 2010; and Benito et al., 2020). The lack of understanding of how uncertainties in
122 palaeoecological data affect the inferences made from them has raised concern (Blaauw
123 2012; Blaauw et al., 2020). We address this knowledge gap by:

- 124 (i) generating multivariate pseudoproxy archives (considered analogous to a
125 time series of proxy data from a core sample);
- 126 (ii) introducing environmental uncertainty to the pseudoproxy archives via
127 simulated core mixing;
- 128 (iii) introducing process and observer error by virtually recreating the
129 observational processes of sub-sampling the core and quantifying proxies
130 from the sub-samples; and
- 131 (iv) applying two multivariate statistical methods independently, Fisher
132 Information (FI; Fisher, 1922) and principal curves (PrC; Hastie and Stuetzle,
133 1989), to analyse the 'error-free' and degraded/sub-sampled data.
- 134 (v) feature analysis methods (a dimensional-reduction method that collapses
135 time-series to a set of metrics) are then applied to the FI and PrCs to quantify
136 the effect of increasing levels of uncertainty

137 Our overarching aim is to quantify the information loss in palaeoecological analyses from
138 environmental uncertainties, and process and observer error, and how this influences
139 statistical analysis and inference using such data. We use FI and PrCs as examples that
140 capture the underlying drivers of a system in different ways. FI captures shorter-term
141 variance e.g., those driven by short-term stochastic processes. PrCs, as a method of indirect
142 gradient analysis, primarily captures the long-term ecosystem trends in the pseudoproxies
143 resulting from the primary driver in the scenarios. A better understanding of how
144 individual and combined sources of uncertainty affect statistical results and interpretation
145 can help inform study design (e.g., determining the number of replicate cores or the sub-
146 sampling resolution needed to detect a signal of interest) and the confidence in the
147 statistical results of a study.

148

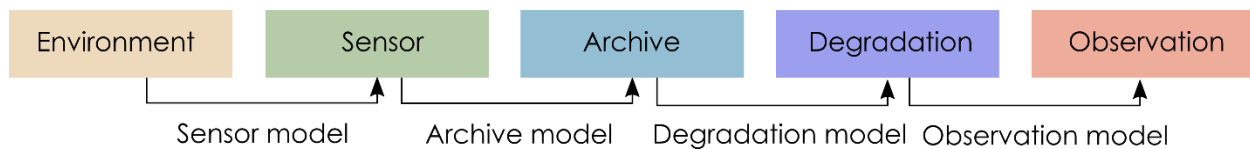
149 **2 Methods**

150 **2.1 Simulating pseudoproxies**

151 Pseudoproxies are simulated using the model described in Asena et al., (2024), following
152 the proxy system model (PSM) framework (Evans et al. 2013) where a sensor (e.g.,
153 terrestrial vegetation) responds to environmental drivers and records that response via
154 proxies (e.g., fossil pollen) counted in an archive such as a lake sediment (in this case a
155 pseudoproxy record). The model we use follows the conceptual framework of a PSM, but is

156 not process-based. We adapt the PSM conceptual framework (Evans et al., 2013) to
157 explicitly include degradation models that describe archive-altering processes before
158 observations are drawn (Figure 1). Asena et al., (2024) describe the three sub-models that
159 generate the pseudoproxy data: (i) a driver model representing the environment in which
160 the archive forms; (ii) a sensor model representing the response of a sensor (e.g.,
161 terrestrial vegetation) to the environment; and (iii) an archive model that represents how
162 the response of the sensor is recorded (e.g., as fossil pollen) in a medium such as a
163 sediment core.

164



165

166 *Figure 1: Adapted Proxy System Model framework (Evans et al., 2013) describing the process*
167 *by which environmental drivers act on a sensor, which records its response in an archive, from*
168 *which observations are drawn. We have included degradation models to describe processes*
169 *acting on the archive before observations are drawn.*

170 'Error-free' pseudo proxies are simulated - in the environment, sensor, and archive sub-
171 models (Figure 1). The model consists of four components: (i) environmental driver change
172 over time (*environment*); (ii) species' niches with respect to the driving environment (the
173 *sensor* response); (iii) pseudoproxy abundances recording the response to driver change in
174 an archive (*archive* record); and (iv) a representation of the formation of the core (*archive*
175 characteristics such as core length and accumulation rate). In summary, the model
176 generates archives of pseudoproxies consisting of 200 potential species representing a
177 palaeoecological record free from the process and observer error associated with empirical
178 data. Pseudoproxy abundances are a response to extrinsic and dynamic environmental
179 drivers with intrinsic variability from disturbance events, introduction to the population
180 via dispersal, and variation in carrying capacity over time. Each species has a tolerance for
181 each environmental driver that, together, defines the species niche and determines the
182 population growth rate of a species at any given time-step as a function of the
183 environmental drivers. If any of the environmental drivers fall outside of a species
184 tolerance to that driver, the species will have a negative growth rate and may eventually
185 become locally extinct. Species that are tolerant of the current environmental conditions
186 can be introduced via dispersal, thus creating a species turnover as conditions change.
187 Simulating 200 species covers a wide range of the driver parameter space and allows
188 different species assemblages to emerge as driver conditions change. Only a subset of the
189 200 species will be presented in the simulated community at any one point in time.

190 Thirty-one replicate models were run for a duration of 5000 time-steps with a burn-in
191 period of 500 time-steps applied to allow species to stabilise with respect to the driving
192 environment. We aimed for a minimum of 30 replicates to account for model variance, and
193 5000 time-steps (c. 5000 years) was sufficiently long to represent ecological turnover in
194 the model. The scenario we present here has two environmental drivers: (i) an abrupt
195 environmental driver switching between constant conditions; and (ii) a random walk

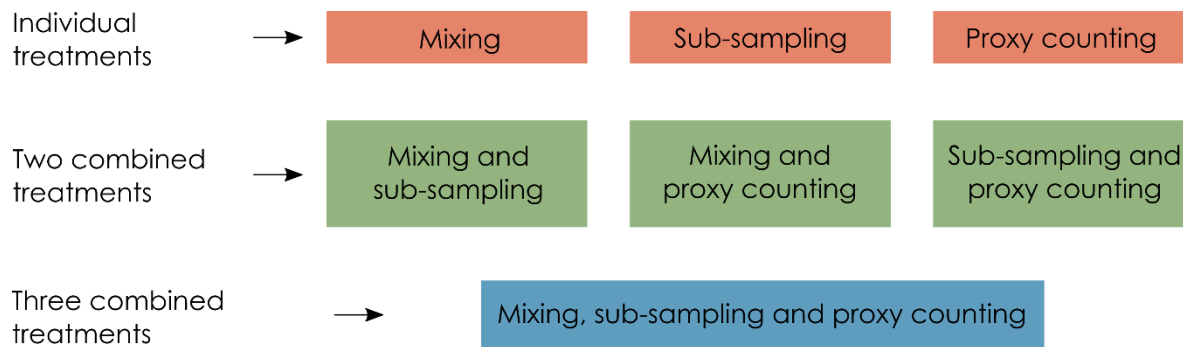
196 driver weighted to 0.15 of the total environmental effect. The magnitude of change in the
197 abrupt driver is insufficient to cause a complete species turnover, and generalist species
198 survive the shift in extrinsic conditions. The random walk driver may amplify or dampen
199 the effects of the abrupt driver, but in general is favourable to most species in the system.
200 The parameters for each species are randomised for each replicate model run around the
201 same baseline parameters (Table S12). The results of an additional three scenarios with
202 different environmental drivers can be found in the supplementary information. We
203 present the abrupt change scenario for two reasons: (i) there are empirical examples of
204 such events (e.g., the termination of the Younger Dryas and the Bølling–Allerød warming;
205 Williams et al., 2011), and (ii) an abrupt shift in community composition is more likely to
206 be detected by statistical analyses. If the statistical methods we assess perform poorly on
207 the abrupt scenario, they are unlikely to perform better on more gradual community
208 turnover.

209

210 Each simulated core is characterised by simulated age, considered to be one year per time-
211 step, and an increase in depth per time-step. The accumulation rate is represented by a
212 combination of a linear decrease with time, with a smoothed random walk superimposed
213 to represent core compression in addition to landscape variability. Variable sedimentation
214 rates result in a different core length (and accumulation per time-step) for each replicate
215 simulation and change the number of model time-steps included in a sub-sample of one-
216 centimetre thickness. Variable change in depth per time-step is calculated as a smoothed
217 and scaled random walk (similar to Benito et al., 2020) representing landscape changes
218 and possible hiatuses. A gradual decrease in depth with age can occur from compaction or
219 compression during extraction (Taranu et al., 2018). The simulated data represent a core-
220 type sample from which sub-samples are taken, proxies quantified, and data analysed
221 similar to real-world core samples. The simulated core is used as an ‘error-free’ benchmark
222 against which methodological and statistical processes are assessed and represents the
223 complete (and un-degraded) absolute abundance of proxy data.

224 **2.2 Degradation and sampling of pseudoproxies**

225 In this section, we describe the degradation model representing post-depositional
226 processes affecting the pseudoproxy data (in this case, core mixing), and the observation
227 models (Figure 1) representing how proxies are quantified from a core sample (here, sub-
228 sampling and the count method applied to micro-fossils on microscope slides). For details
229 and visualisations of the degradation models, see Asena et al., (2024). We apply three
230 treatments to each of the model replicates: mixing (degradation), sub-sampling and proxy
231 counting (observation), applied at 10 levels each individually and combined (Figure 2).
232 Together, the degradation and observation models represent process- and observer-
233 introduced error that affect the data before quantitative analyses are applied. Each of the
234 31 replicate archives results in 1210 datasets from the ‘error-free’ reference core to the
235 most uncertain.



236

237 *Figure 2: Each uncertainty (treatment) is applied to the 'error-free' pseudoproxy archive to*
 238 *systematically introduce uncertainty individually, and in combination.*

239

240 2.2.1 Virtual mixing: degradation model

241 Core mixing is applied as a centrally weighted rolling-average over time-windows of the
 242 archive ranging from unmixed (the 'error-free' benchmark) to a window of 10 time-steps.
 243 Simulated mixing is represented as consistent over time, rather than being a depth-
 244 dependent process such as bioturbation.

245 2.2.2 Virtual sub-sampling: observation model

246 An absolute proxy abundance per time-step is generated by the model and is sub-sampled
 247 at regular depth intervals ranging from one to ten centimetres. Each sub-sample has a
 248 thickness of one centimetre; the number of time-steps spanned by the sampled thickness is
 249 determined by the simulated accumulation rate. If the one-centimetre sub-sample covers
 250 multiple time-steps, the proxy abundances in that sub-sample are summed. All sub-sample
 251 treatment data are converted to relative abundances before analysis so that the analyses
 252 are not influenced by excessive values from the summed proxies of multiple time-steps.
 253 When applied in combination with simulated proxy counting, values are converted to
 254 relative abundance after the proxy count treatment.

255 2.2.3 Virtual proxy count: observation model

256 The process of counting proxies in a sub-sample (e.g., counting several hundred pollen
 257 grains or diatoms on a microscope slide) is simulated by random sampling from the
 258 absolute proxy abundances with resolutions increasing from 100 to 1000 by 100. The
 259 probability of a proxy occurring in the random sample is based on the abundance of that
 260 proxy. The sample is then converted to relative abundances comparable to empirical proxy
 261 data. The simulated count treatment is applied to the raw, mixed, and sub-sampled data.
 262 Increasing levels of uncertainty in the proxy counting treatment are represented by a
 263 decrease in the proxy count resolution.

264 2.3 Quantitative analyses

265 After the application of the degradation and observation models, the pseudoproxy data
 266 span a gradient of uncertainty from the 'error-free' data to the uncertain data that reflect

267 what we observe from a system. We then apply statistical analyses along this gradient to
 268 determine the influence of each source of uncertainty (the penultimate step of the VE
 269 approach). FI and PrCs are used to analyse each treatment level from each replicate core
 270 (treatment level being the severity of each of the treatments, mixing, sub-sampling and
 271 proxy counting). FI and ordination methods have been suggested as appropriate where
 272 there are an unlimited number of input variables of any data type that do not require *a*
 273 *priori* knowledge of the driving state variables of a system (Roberts et al., 2018). The FI and
 274 PrC produce a large amount of data, so we use feature analysis for time-series (FATs; Nun
 275 et al., 2015) to synthesise them and reduce each time-series to a small number of metrics
 276 (or ‘features’) that we can compare across treatment levels (detailed below). Each replicate
 277 core results in 1210 FI time-series and PrCs, and by extracting a set of features, the
 278 difference among treatment levels can be calculated as a measure of distance, we use
 279 Euclidean distance. The data analysis process is as follows: (i) calculate FI and PrC for each
 280 treatment level; (ii) extract features from the FI and PrC outputs; and (iii) calculate the
 281 distance between the features of each treatment level (Figure 3).

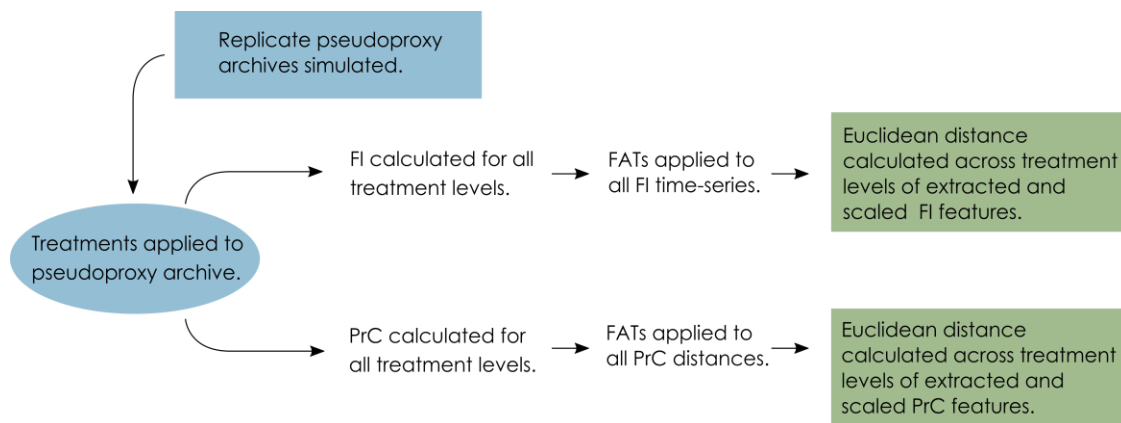


Figure 3: Conceptual data-flow of the degradation, sampling and analysis process. Treatments of mixing, sub-sampling and proxy counting are applied individually and in combination to the replicate pseudoproxy archives (Figure 2). Fisher information (FI) and principal curves (PrC) are applied separately to each treatment and subsequently analysed using feature analysis for time-series (FATs). Extracted features are scaled and Euclidean distance between each treatment level and the ‘error-free’ reference core is calculated.

282 2.3.1 Fisher Information (FI)

283 Fisher information was developed to quantify information about an unknown parameter
 284 from measurable variables (Fisher, 1922) and has since been used as a measure of
 285 ecosystem stability (Cabezas and Fath, 2002; Mayer et al., 2006; Karunanithi et al. 2008;
 286 Eason et al., 2016). Fisher information has been applied to palaeoecological data, with the
 287 suggestion that it can be used as an indicator of an approaching regime shift, such as a shift
 288 in diatom species’ composition (Spanbauer et al., 2014). Fundamentally, FI evaluates the
 289 probability of detecting different system states over time, or the ‘stability’ of the system;
 290 thus, FI changes with the variance in the system. Pseudoproxies from each replicate core,

291 and each level of uncertainty, are analysed using FI, using a custom R package (Asena et al.,
292 2023).

293 *2.3.2 Principal curves*

294 Principal curves can be used to identify the underlying variables (e.g., a steadily changing
295 variable over time) that describe a system characterised by multiple state variables and can
296 be considered as a form of non-linear principal components analysis (De'ath, 1999). In
297 short, a PrC is a one-dimensional curve fit through the 'middle' of an n -dimensional space
298 (e.g., species composition data; Hastie and Stuetzle, 1989). The curve represents species
299 compositions by mapping (or projecting) the sites, e.g., the species' composition at a given
300 sample, onto a low-dimensional space, and using similarity or dissimilarity measures to
301 measure the distance between sites (assessing, for example, the species' compositional
302 change through time). The arrangement of sites reflects the composition of species in the
303 reduced dimension space as the distance between sites is proportional to the distance in
304 species composition (De'ath, 1999). Principal curves can be used as a method of gradient
305 analysis, the underlying concept being that the species abundances change in a predictable
306 way along an ecological gradient. Here, we use PrCs to represent change in species
307 composition over time and as a method of indirect gradient analysis using the distances
308 along the PrC. Cubic smoothing splines are used to fit the PrC to the data. Hastie and
309 Stuetzle (1989), De'ath (1999), and Simpson and Birks (2012) detail the implementation of
310 PrCs. PrC analyses were conducted for all replicate pseudoproxy datasets for each level of
311 increasing uncertainty using the analogue package (Simpson and Oksanen, 2020) in R (R
312 Core Team 2020).

313 *2.4 Assessing results: Feature analysis for time-series*

314 The final step of the VE approach is to assess the outcomes of the statistical analyses
315 applied to the degraded and sampled data against the 'error-free' pseudoproxies. To
316 compare the FI and PrC time-series across treatment levels, we use feature analysis.
317 Feature analysis is a method of reducing a two-dimensional time-series to a one-
318 dimensional set of 'features'. Features are metrics that describe a time-series in terms of
319 summary statistics (e.g., mean and variance), and more complicated descriptors such as
320 autocorrelation length (Nun et al., 2015). We developed a set of 62 features (Table SI4)
321 drawing on feature analysis for time-series (Richards et al., 2011; Kim et al., 2011; Nun et
322 al., 2015; Sokolovsky et al., 2017) and change point analysis (Killick and Eckley, 2014). The
323 individual and combined degradation and sampling treatments result in 1210 time-series
324 per replicate, yielding $31 \times 1210 = 37510$ virtual cores per scenario. Describing the FI time-
325 series and PrC as a series of features allows comparison between the 1210 treatments by
326 calculating a distance measure (we use Euclidean distance) between the extracted features
327 of each treatment level. The feature analysis process is as follows:

- 328 1. Features are extracted from the FI time-series and distances along the PrCs for all
329 replicate model runs of the 'error-free' archive.
- 330 2. A correlation matrix of the features from the replicate 'error-free' datasets is
331 constructed, and features with a Pearson's correlation coefficient greater than $|0.7|$
332 are excluded sequentially, recalculating the correlation matrix until all highly

333 correlated features are dropped, starting with the highest correlation coefficient
334 (Dormann, et al. 2007).

- 335 3. The remaining features (with a Pearson's correlation coefficient less than |0.7|) are
336 then calculated for all replicates across all treatment levels, resulting in a number
337 (ranging between 14-26 per scenario) of single metric features per treatment that
338 describe the FI time-series and PrC.
- 339 4. The features are scaled (by subtracting the mean of the entire series from each point
340 and dividing it by the series' standard deviation), and the Euclidean distance is
341 calculated across treatment levels, resulting in a single distance measure between
342 the 'error-free' core and each treatment level.
- 343 5. Summaries of the Euclidean distances are calculated for all treatment levels across
344 replicates, resulting in a single distance measure for each treatment from the 'error-
345 free' benchmark.

346

347 **3 Results**

348 **3.1 Effects of individual sources of uncertainty**

349 In the extracted features for FI, sub-sampling causes the largest overall increase in the
350 median Euclidean distance from the 'error-free' core, followed by proxy counting and then
351 mixing; however, there is overlap in the confidence envelopes across all three treatments
352 (Figure 4A). Distance from the 'error-free' core increases consistently with uncertainty in
353 the mixing treatment, showing a steeper increase in distance across uncertainty compared
354 with the other two treatments. Between successive treatment levels, proxy counting shows
355 little increase in the median Euclidean distance as uncertainty increases. In the sub-
356 sampling treatment, distance increases more in the lower uncertainty levels than in the
357 higher levels, plateauing somewhat at higher uncertainty (Figure 4A). There is some
358 variability across the treatment levels resulting from the stochasticity in the underlying
359 model and simulated observational processes (i.e., proxy counting is a random sampling
360 process, and sub-sampling is dependent on the variable accumulation rates of the core).

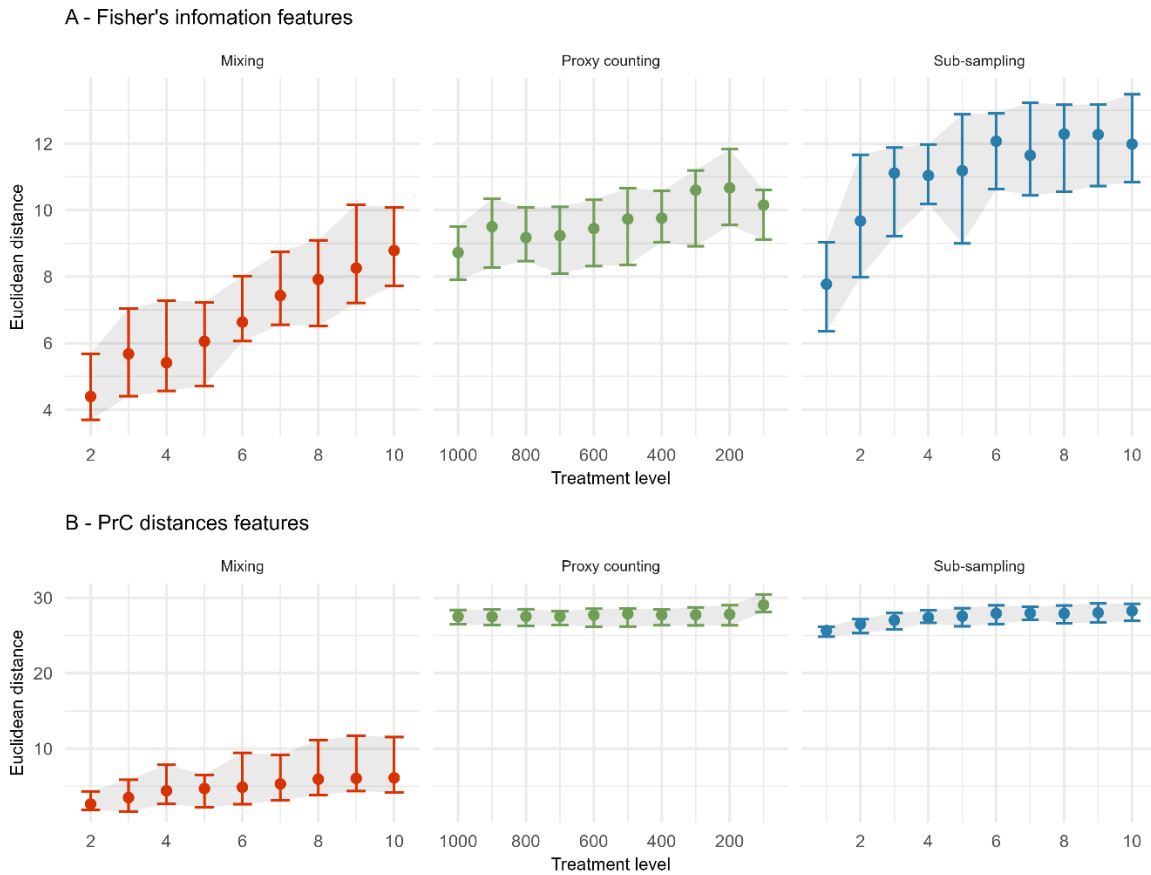


Figure 4: The median (dots), 25th, and 75th quantiles (error-bars and shaded area) of the Euclidean distance from the 'error-free' core of features extracted from the Fisher information (A) and PrC distances (B) calculated across replicate simulations. Note the x-axis is organised so uncertainty consistently increases from left-to-right.

361 For the PrC features, across all scenarios the mixing treatment has the least effect on
 362 median Euclidean distance (Figure 4B). Proxy counting and sub-sampling have overlapping
 363 confidence envelopes, although they are much smaller than those of the mixing treatment.
 364 Proxy counting shows no consistent pattern in median Euclidean distance between
 365 successive treatment levels until the lowest count resolution. Conversely, the sub-sampling
 366 treatment shows an increase in the lower treatment levels, plateauing as sub-sampling
 367 interval increases (Figure 4B).

368

369 3.2 Effects of two combined sources of uncertainty

370 In the following section, treatments are applied simultaneously to determine which
 371 combinations cause the greatest effect on analyses of the core. The greatest increase in
 372 mean Euclidean distance on the features extracted from FI from the 'error-free' core arises
 373 from the interaction of the sub-sampling and proxy counting uncertainties increasing

374 together (i.e., along the diagonal; Figure 5A), with a stronger effect from the subsampling
375 treatment. Mixing combined with sub-sampling or with proxy counting shows no clear
376 interaction effect as the treatments increase in severity together. The smallest increase in
377 distance is from the combination of mixing with proxy counting, suggesting that sub-
378 sampling tends to have the greatest influence of the three treatments (Figure 5A). The
379 effect of the mixing treatment on the mean Euclidean distance is small when compared to
380 those of either sub-sampling or proxy counting (Figure 5A). Variability across the surface of
381 each plot emerges from underlying model stochasticity, random sampling in the simulated
382 count method, and the variable accumulation rates of the replicate cores.

383

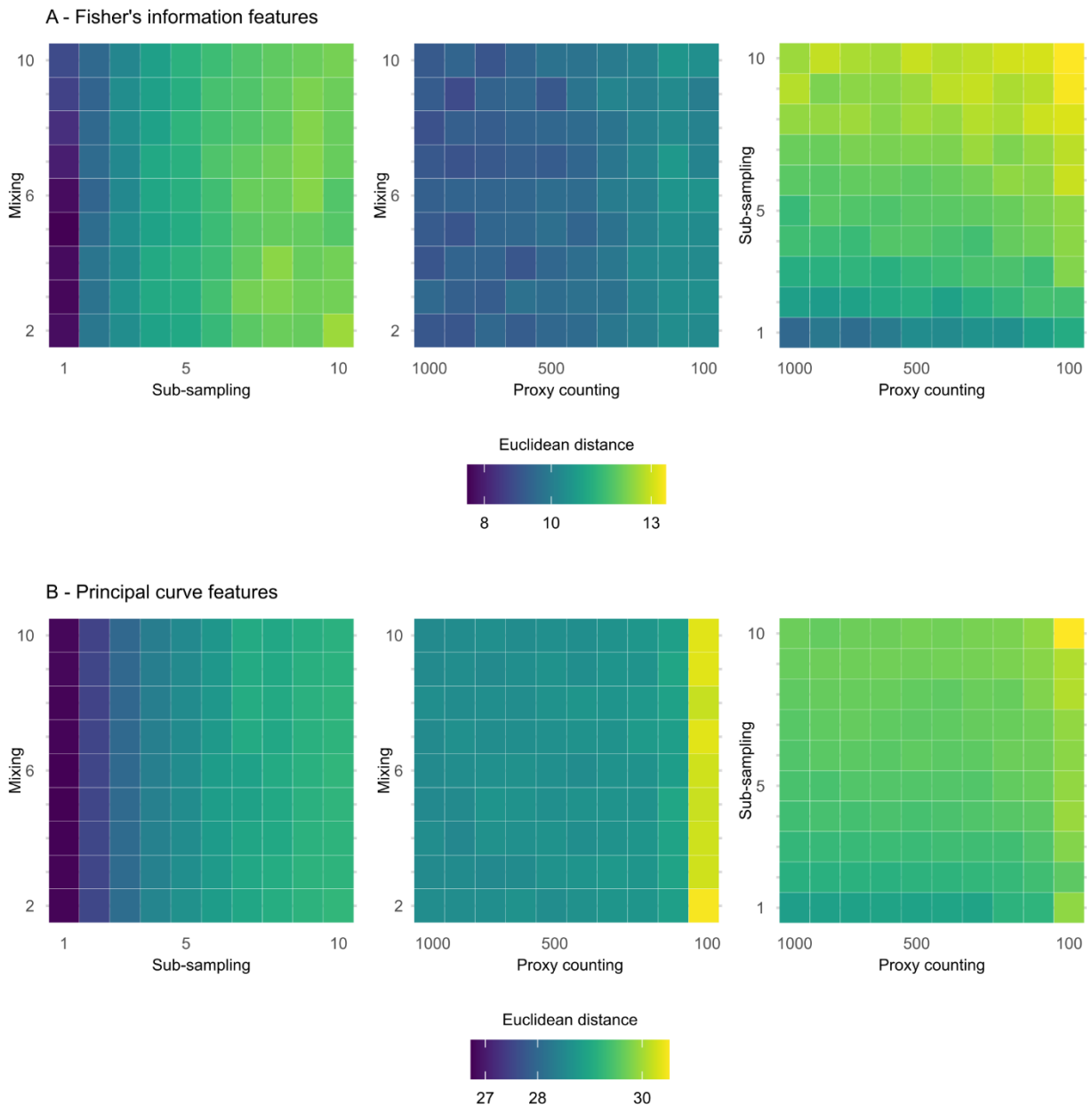


Figure 5: Mean Euclidean distance of features from the 'error-free' core of two treatments combined calculated across replicate simulations for Fisher information (A) and principal curves (B). The mixing axis shows the number of time-steps over which mixing occurs. Along the sub-sampling axis, the frequency of sub-sampling in centimetres is shown, and the proxy counting axis displays count resolutions in number of individuals counted per sample. In the proxy counting treatment, uncertainty increases as count resolution decreases.

386 In the extracted features from the distances along the PrCs, the combined effects of sub-
 387 sampling with proxy counting show the largest increase in the mean Euclidean distance of
 388 all the combined treatments, with a weak interaction effect as proxy count and sub-
 389 sampling uncertainties increase together (Figure 5B). No interaction effect is visible in
 390 either the combined treatments of mixing with sub-sampling or mixing with proxy
 391 counting (Figure 5B).

392 3.3 Effects of three combined sources of uncertainty

393 Interaction effects of all three uncertainties applied simultaneously were assessed for the
 394 extracted FI and PrC features (Figure 6). An interaction effect is visible in the increase of
 395 mean Euclidean distance as the sub-sampling interval increases (along the x-axis), together
 396 with proxy counting resolution decreasing (across facets from top left to bottom right);
 397 however, no clear increase is visible along the mixing axis, indicating little contribution
 398 from mixing to the interaction of the three treatments (Figure 6). Overall, the greatest
 399 increase in the mean Euclidean distance among treatments is at the lowest proxy count and
 400 largest sub-sampling interval.

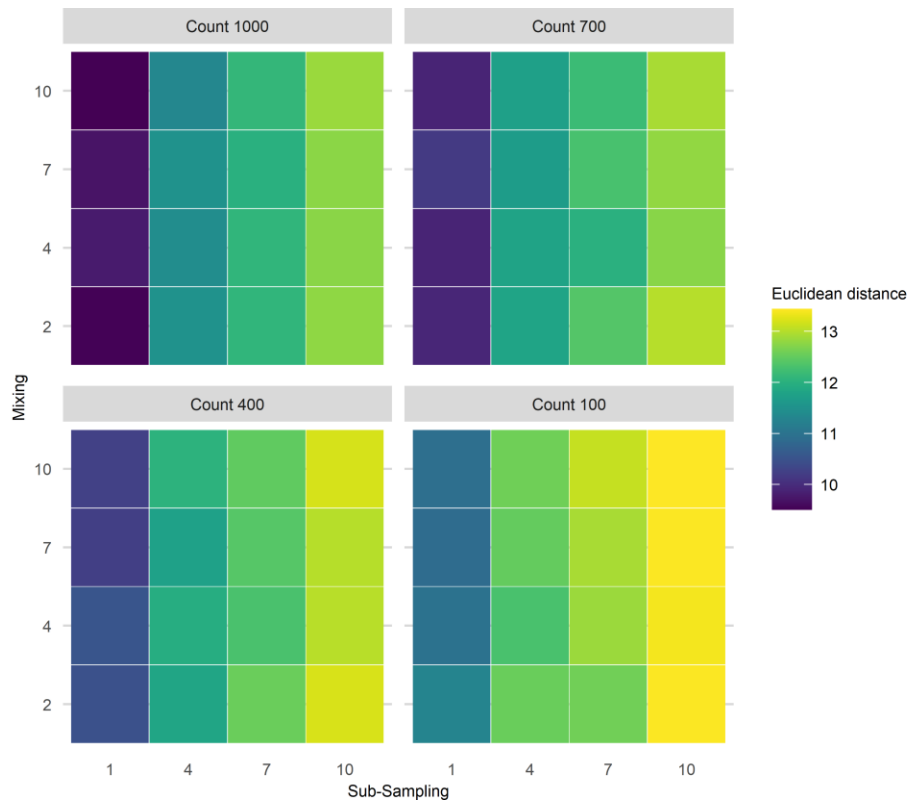


Figure 6: Mean Euclidean distance of Fisher's Information from the 'error-free' core for three treatments applied in combination. To demonstrate the three treatment dimensions, results are displayed such that each plot axis shows mixing (number of time-steps over which mixing occurs) and sub-sampling (frequency in centimetres) treatments, and each facet (sub-plot) is the proxy counting treatment (number of individuals counted in sub-sample). Uncertainty from proxy counting increases from the top left to the bottom right.

401 In the PrC features, applying three treatments in combination does not show a clear three-
 402 way interaction as uncertainty increases (Figure 7). An increase in mean Euclidean
 403 distance is visible along the sub-sampling axis (as sub-sampling interval increases), but
 404 there is little visible effect of the proxy counting treatment (reducing in resolution across
 405 facets from top left to bottom right) until the lowest resolution. Mixing contributes
 406 relatively little to the overall increase in mean Euclidean distance showing no visible
 407 increase along the mixing axis (Figure 7).

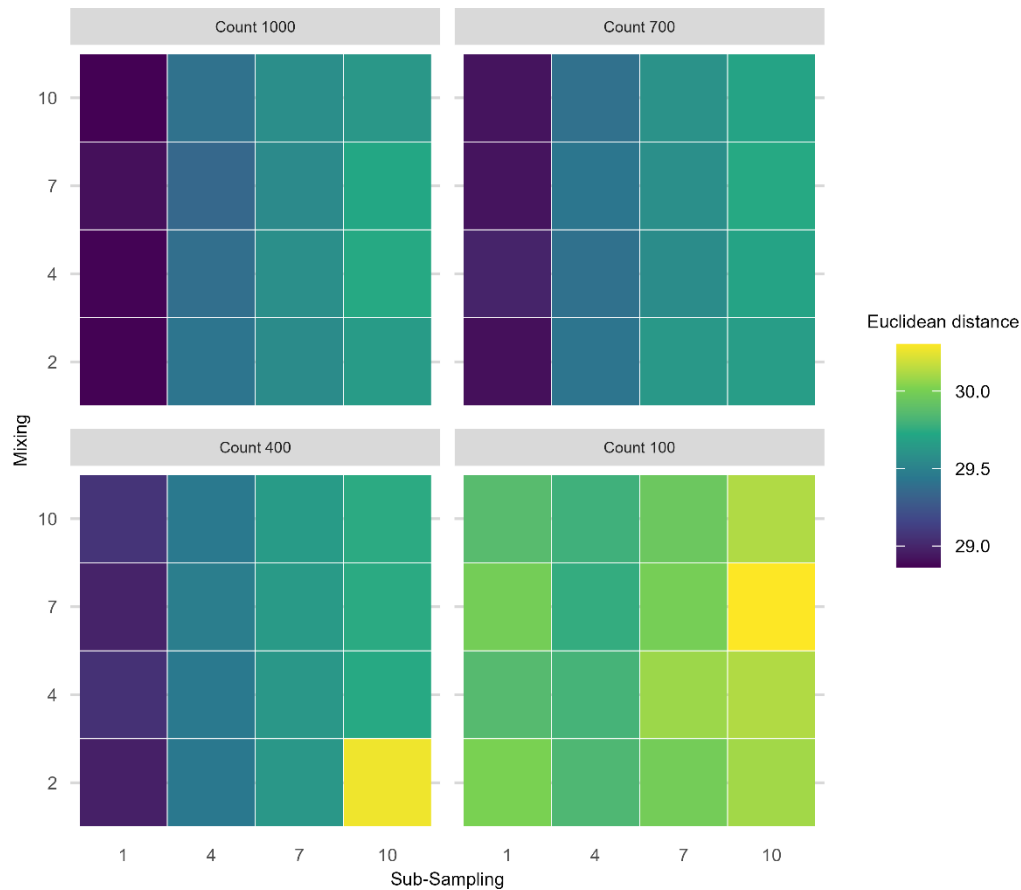


Figure 7: Mean Euclidean distance of the principal curves from the 'error-free' core of all uncertainties increasing in combination. Same plot layout and interpretation as Figure 6.

408 4 Discussion

409 To draw reliable conclusions from palaeoecological data, it is crucial to view our inferences
 410 in the context of the uncertainties they integrate. Our goal in this paper was to address
 411 how process and observer error affect statistical methods applied to palaeoecological data
 412 and the inferences we draw from them. Here, we have assessed some of the uncertainties
 413 that affect species proxy data. Additionally, uncertainty arises from building chronologies
 414 (Blaauw et al., 2018; Parnell et al., 2008; Telford et al., 2004) and measuring abiotic system
 415 variables, such as isotopic records and lake level reconstructions, which carry their own
 416 uncertainties.

417 **4.1 Effects of individual sources of uncertainty**

418 Without exception, sub-sampling treatments show the largest effect on the median
419 Euclidean distances of the FI features (with some overlap in the confidence envelope with
420 the proxy counting treatment), followed by the proxy counting process. For the PrC
421 features, both sub-sampling and proxy counting treatments had a similar effect on
422 Euclidean distance. For both the FI and PrC features, the smallest effect on Euclidean
423 distance between the 'error-free' and degraded cores came from the simulated mixing
424 degradation process.

425 Perhaps the most interesting implication of our analyses in the context of empirical ecology
426 is how the effects of sources of error differ between the two statistical metrics (FI and PrC).
427 Beyond the initial increase in Euclidean distance in the PrC from the application of proxy
428 counting and sub-sampling (an unavoidable cost), there was little further effect until the
429 lowest proxy count and sub-sampling resolutions. Thus, PrCs may be a useful measure of a
430 system's trajectory for patchy data (e.g., initial analysis of low sub-sampling resolution data
431 before deciding where to focus sampling effort). For FI, treatment effects have a more
432 consistent increase in distance from the 'error-free' core with treatment intensity. The
433 short-term variability captured by FI may provide useful system indicators (*sensu* Eason
434 and Cabezas, 2012) but may also require high-quality data (e.g., high sub-sampling
435 resolution and proxy counting) for reliable inferences. The required temporal resolution of
436 the data is also likely to increase if accumulation rates are slow and species turnover is
437 rapid. Increased sub-sampling frequency is required in systems that change rapidly
438 compared with more stable systems where the difference between successive time-steps is
439 small. Slow accumulation rates mean that a one-centimetre-thick sub-sample integrates
440 multiple years of ecological change; thus, uncertainty from sub-sampling resolution will
441 increase if the accumulation rate is slow and ecological change is rapid. An observer may
442 interpret FI results with the knowledge of which sources of uncertainty, whether
443 controllable (e.g., sub-sampling and proxy counting resolution) or uncontrollable (e.g.,
444 mixing and accumulation rates), have the greatest influence. After introducing
445 uncertainties to the pseudoproxies, the primary patterns, such as long periods of increase
446 in FI, remain visible and offer a useful depiction of community change.

447 **4.2 Effects of combined sources of uncertainty**

448 For both FI and PrC, when two treatments are applied in combination, the greatest overall
449 increase in mean Euclidean distance from the 'error-free' core resulted from sub-sampling
450 uncertainty in combination with proxy counting uncertainty. For the PrC the maximum
451 increase in mean Euclidean distance for two simultaneous treatments occurred at the
452 lowest proxy count resolution in combination with mixing, but such a low proxy count
453 resolution is unlikely in any empirical study. In our analyses, mixing has relatively little
454 effect compared with sub-sampling or proxy counting, and the effect tends to be obscured
455 by other sources of stochasticity (disturbance, dispersal, and temporal changes in carrying
456 capacity), variable accumulation rates, and randomised sampling of the proxy abundances.
457 Similarly, when three sources of uncertainty are combined, mixing shows the least effect,
458 and no apparent interaction with sub-sampling or proxy counting. However, it is worth
459 noting, that our implementation of mixing is relatively simple in that the effect on the

460 pseudoproxy data is a centrally weighted smoothing. More extreme mixing, and time-
461 varied mixing effects are likely to show a stronger effect.

462 In the case of FI, the greatest benefit in terms of reducing the distance from the 'error-free'
463 core came from increasing sub-sampling resolution followed by proxy count resolution.
464 However, from the standpoint of an observer, increasing the resolution of an FI time-series
465 may not increase the information content, at least in terms of capturing long-term patterns.
466 Simple driving environments (e.g., the single driver simulations) are likely to be adequately
467 represented by FI applied to low-resolution data; however, interpretation of FI from
468 environments influenced by multiple drivers is potentially challenging without
469 considerable knowledge of the underlying driving conditions. The benefit of the VE
470 approach is that it allows us to examine how the underlying dynamics manifest in
471 multivariate indicators of change, such as FI; however, such near-complete information is
472 rarely, if ever, available. Ultimately, an observer must base sampling and analysis decisions
473 on their specific aims. If accurate evaluation of short-term variability is a goal (e.g., for
474 studies of ecosystem resilience), then dedicating resources to sub-sampling resolution is
475 likely to be beneficial to analyses such as FI. Reducing observer error, a more controllable
476 source of error, may help detect a short-term signal of interest if the uncontrollable sources
477 of error, such as sediment accumulation rates, mixing, and driver variability, are
478 sufficiently small that the signal remains detectable.

479 PrC shows little increase in distance (after the initial increase from the application of the
480 treatments) from the 'error-free' reference with combined treatment levels. Thus, as a
481 representation of compositional change, it may be robust to low-resolution data (e.g.,
482 infrequent sub-sampling). Short-term changes in abundance (e.g., small disturbances) will
483 likely become less evident in the PrC; however, our results suggest that overall patterns
484 seen in a PrC are robust to multiple sources of error. Thus, from the perspective of an
485 observer, high-resolution data may only be required for PrC to identify short-term
486 compositional changes, such as perturbations that take a few generations to recover from.

487 **4.3 Lessons from virtual ecology for empirical studies**

488 Using virtual ecology to estimate the influence of sources of uncertainty on quantitative
489 analyses helps us to understand what can be done to mitigate their effects and where to
490 focus limited resources, such as time spent analysing an individual core. Trade-offs are
491 inherent in any sampling design. For example, is it more advantageous to focus effort on
492 spatial coverage by taking multiple cores rather than increasing sub-sampling resolution
493 on fewer cores? Such questions, of course, depend on the intention of the study and
494 knowledge of the study site/system (i.e., some knowledge of the uncertainties that will be
495 encountered, such as landscape changes through time). Virtual ecology allows us to make a
496 more informed decision about what field and laboratory methods, and quantitative
497 analyses will be most appropriate given the question of interest. For example, if analysing a
498 network of core data over a large geographic region, where the observer is interested in the
499 spatial consistency of the system's trajectory but there are not the resources to extract
500 highly resolved data from each core, methods such as PrC may be more informative than FI.
501 Conversely, if an observer is interested in short-term change in a single core (or a region of
502 particular interest in a core), it may be worth allocating the time to extracting highly

503 resolved data to increase the reliability of analyses sensitive to variance such as FI. PrC and
504 FI provide different representations of a system's trajectory. Principal curves reflect the
505 system's overall trajectory (De'ath, 1999) and, as a form of indirect gradient analysis, PrC
506 reflects the primary driver of the scenario. In contrast, FI is more sensitive to short-term
507 variability (Eason et al., 2016) and so reflects driver interactions. Although FI does capture
508 the long-term system trajectory, these trends can be obscured by short-term variability
509 such as that caused by the random walk driver. Similar analyses (e.g., other ordination
510 methods) may be affected by sources of uncertainty in similar ways. Of course, FI and PrC
511 are only two of a suite of available statistical analyses (Birks et al. 2012; Blaauw et al.,
512 2020), and an observer should apply more than one.

513 Alongside considerations of the sensitivity of analyses to uncertainty, there are questions of
514 how sensitive different proxies are to driver change and, consequently, how informative
515 the analyses are. The question of how different proxies respond to drivers at different
516 temporal and spatial scales (e.g., Wilmshurst et al., 2002) remains poorly resolved.
517 Interestingly, the sensitivity of different proxies to environmental change may be
518 ecosystem-specific. Phytoliths have been reported as more sensitive than pollen to changes
519 in dry forests, with the reverse being true of evergreen forests at a site in Bolivia
520 (Plumpton et al., 2019). In savannahs, pollen and phytoliths are equally sensitive to
521 changes in the environment (Plumpton et al., 2019). Thus, ecosystem-specific and proxy-
522 specific knowledge are important considerations, as increasing sub-sampling efforts to
523 obtain a higher resolution representation of change from numerical analyses may not be
524 useful if the proxy is not a reliable sensor at that resolution. Furthermore, compositional
525 change is not the sole (or necessarily the most appropriate) measure of system change, and
526 other descriptors such as body-size distributions, physiognomic, and functional and
527 phylogenetic diversity can be included (Goring et al., 2013; Reitalu et al., 2015; Clements
528 and Ozgul, 2016; Spanbauer et al., 2016; Adeleye et al., 2023).

529

530 The advantage of using a phenomenological modelling approach designed to mimic the
531 statistical properties of empirical data, is that the results are informative without
532 attempting to recreate species abundances of a specific system and addressing the
533 challenges faced by more process-based models. Our model and virtual approach can be
534 used to assess, for example, the performance of statistical methods, the influence of
535 observational and chronological uncertainty, and explore a range of driving environments.
536 It becomes possible to address questions such as 'what statistical method is likely to be
537 appropriate for my data and research question?' However, without recreating a specific
538 system, it cannot answer questions such as 'should I use a 2 or 4 cm resolution sub-
539 sampling procedure for this core?'. To answer such questions, process-based VE
540 approaches are necessary. Of course, process-based models face numerous challenges of
541 accurately representing mechanisms and being able to reasonably recreate a given system
542 to address such questions. The VE approach can be applied using process-based models to
543 generate data, or simulating data from a statistical model fit to the empirical data, and
544 following the same process of degrading, sub-sampling and fitting/re-fitting, to assess how
545 parameters change.

546 Finally, we can consider, empirical, experimental, semi-empirical approaches to advance
547 our understanding of uncertainties in palaeoecology. Empirical approaches could involve
548 collecting high-quality data (e.g., well-dated sediment cores with frequent sub-sampling
549 resolution), ideally with replicate cores from the same location, to use as a benchmark
550 against which to assess analyses when sub-sampling resolution is reduced (e.g., Liu et al.,
551 2012). Experimental approaches might include laboratory and *in situ* manipulation; for
552 example, Payne and Gehrels (2010) monitor the movement of tephra in the field and under
553 controlled laboratory environments to understand the influence of tephra taphonomy on
554 tephrochronology. Semi-empirical approaches would combining empirical-virtual methods
555 could be developed using (virtually) modified empirical data; for example, applying a
556 simulated mixing process to empirical sediment core data (such as those from varved
557 sediments that are subject to minimal mixing) and assessing the subsequent analyses.
558 Mann and Rutherford (2002) demonstrate this approach by generating pseudoproxy data
559 by subjecting instrumental data to degradation, such as various noise processes and spatial
560 sampling strategies, to assess sea surface temperature reconstruction methods. They used
561 simulation to create a continuous sea surface temperature record from the patchier
562 instrumental data before applying the degradation processes. Although the implications of
563 such methods are different for ecological data, similar approaches could fruitfully be
564 applied.

565

566 **5 Conclusion**

567 Palaeoecological uncertainty can be considered at four levels: environmental processes,
568 field methods, laboratory methods, and quantitative analyses (Table 1). The effects of
569 different sources of uncertainty are challenging to disentangle and quantify from empirical
570 studies alone, and virtual ecology provides a useful approach as different uncertainties can
571 be manipulated. However, virtual ecology has its own set of limitations. The data
572 degradation and sampling processes described here still represent a relatively ideal
573 situation in that the timespan of the data is long relative to the driving processes, and the
574 sub-sampling treatment is at regular depth intervals for example. Thus, investigation of
575 uncertainty through both empirical and virtual approaches is necessary to better
576 understand the influence of process and observer error on the analysis of palaeoecological
577 data. A better understanding of the how different proxies record environmental signals in
578 an archive (e.g., how closely coupled a signal recorded by a proxy data is to the
579 environmental change) and the uncertainties around quantifying and analysing proxy data
580 can bring us closer to understanding long-term climate and ecosystem dynamics. Although
581 we have assessed sources of uncertainty on pseudoproxy data representing species
582 communities, all proxies such as isotopic data, or tree ring data, have their own
583 idiosyncratic sources of uncertainty. Virtual Ecological approaches can help towards
584 assessing their uncertainties.

585

586

587 **Acknowledgements**

588 The authors are very grateful for the support of the Centre for eResearch, University of
589 Auckland particularly Nick Young and Noel Zeng for their digital research expertise. We
590 also acknowledge the New Zealand eScience Infrastructure (NeSI) for the use of their
591 computational resources, without which the scale of the analyses involved in this paper
592 would not have been possible. Callum Walley and Anthony Shaw of NeSI provided
593 instrumental support for high-performance computing. Finally, we extend our thanks to
594 members of the Perry Lab for helping shape the project.

595 **Data availability**

596 Functions used to compute Fisher Information and the derived metrics can be found here:
597 <https://doi.org/10.5281/zenodo.8052806>. Additional functions used to calculate metrics
598 from principal curves can be found here: <https://doi.org/10.5281/zenodo.18200665>.

599

600 **Author contributions**

601 Quinn Asena contributed to the conceptualization, methodology, and writing the original
602 draft. George Perry contributed to the conceptualization, methodology, and reviewing and
603 editing the manuscript, providing supervision and statistical expertise. Janet Wilmshurst
604 provided palaeoecological expertise to the project, and reviewed and edited the
605 manuscript.

606

607 **Funding**

608 The author(s) disclosed receipt of the following financial support for the research,
609 authorship, and/or publication of this article: This work was conducted through the New
610 Zealand's Biological Heritage National Science Challenge, which is funded by the New
611 Zealand Ministry of Business, Innovation and Employment.

612

613 **References**

614 Adesanya Adeleye, M., Charles Andrew, S., Gallagher, R., van der Kaars, S., De Deckker, P.,
615 Hua, Q., Haberle, S.G., 2023. On the timing of megafaunal extinction and associated floristic
616 consequences in Australia through the lens of functional palaeoecology. *Quaternary Science*
617 *Reviews* 316, 108263. <https://doi.org/10.1016/j.quascirev.2023.108263>

618 Asena, Quinn, George LW Perry, and Janet M Wilmshurst. 2024. "Is the Past Recoverable
619 from the Data? Pseudoproxy Modelling of Uncertainties in Palaeoecological Data." *The*
620 *Holocene*, May, 09596836241247304. <https://doi.org/10.1177/09596836241247304>.

- 621 Asena, Quinn, Nick Young, and Alex Pletzer. 2023. "UoA-eResearch/fisheR: V1.0.0." Zenodo.
622 <https://doi.org/10.5281/ZENODO.8052806>.
- 623 Beck, Kristen K., Michael-Shawn Fletcher, Patricia S. Gadd, Henk Heijnis, Krystyna M.
624 Saunders, Gavin L. Simpson, and Atun Zawadzki. 2018. "Variance and Rate-of-Change as
625 Early Warning Signals for a Critical Transition in an Aquatic Ecosystem State: A Test Case
626 from Tasmania, Australia." *Journal of Geophysical Research: Biogeosciences* 123 (2): 495–
627 508. <https://doi.org/10.1002/2017JG004135>.
- 628 Benito, Blas M., Graciela Gil-Romera, and H. John B. Birks. 2020. "Ecological Memory at
629 Millennial Time-Scales: The Importance of Data Constraints, Species Longevity and Niche
630 Features." *Ecography* 43 (1): 1–10. <https://doi.org/10.1111/ecog.04772>.
- 631 Birks, John B. H., André F. Lotter, Steve Juggins, and John P. Smol. 2012. *Tracking*
632 *Environmental Change Using Lake Sediments: Data Handling and Numerical Techniques*.
633 Springer Science & Business Media.
- 634 Blaauw, Maarten. 2012. "Out of Tune: The Dangers of Aligning Proxy Archives." *Quaternary*
635 *Science Reviews, The INTegration of Ice Core, Marine and TERrestrial Records of the Last*
636 *Termination (INTIMATE)* 60,000 to 8000 BP, 36 (March): 38–49.
637 <https://doi.org/10.1016/j.quascirev.2010.11.012>.
- 638 Blaauw, Maarten, K. D. Bennett, and J. Andrés Christen. 2010. "Random Walk Simulations of
639 Fossil Proxy Data." *The Holocene* 20 (4): 645–49.
640 <https://doi.org/10.1177/0959683609355180>.
- 641 Blaauw, Maarten, J. Andrés Christen, and Marco Antonio Aquino-López. 2020. "A Review of
642 Statistics in Palaeoenvironmental Research." *Journal of Agricultural, Biological and*
643 *Environmental Statistics* 25 (1): 17–31. <https://doi.org/10.1007/s13253-019-00374-2>.
- 644 Bothe, Oliver, Sebastian Wagner, and Eduardo Zorita. 2019. "Simple Noise Estimates and
645 Pseudoproxies for the Last 21000 Years." *Earth System Science Data* 11 (3): 1129–52.
646 <https://doi.org/10.5194/essd-11-1129-2019>.
- 647 Cabezas, Heriberto, and Brian D. Fath. 2002. "Towards a Theory of Sustainable Systems."
648 *Fluid Phase Equilibria*, Proceedings of the Ninth International Conference on Properties and
649 Phase Equilibria for Product and Process Design, 194–197 (March): 3–14.
650 [https://doi.org/10.1016/S0378-3812\(01\)00677-X](https://doi.org/10.1016/S0378-3812(01)00677-X).
- 651 Christiansen, Bo, T. Schmith, and P. Thejll. 2009. "A Surrogate Ensemble Study of Climate
652 Reconstruction Methods: Stochasticity and Robustness." *Journal of Climate* 22 (4): 951–76.
653 <https://doi.org/10.1175/2008JCLI2301.1>.
- 654 Clements, Christopher F., and Arpat Ozgul. 2016. "Including Trait-Based Early Warning
655 Signals Helps Predict Population Collapse." *Nature Communications* 7 (1).
656 <https://doi.org/10.1038/ncomms10984>.

- 657 De'ath, Glenn. 1999. "Principal Curves: A New Technique for Indirect and Direct Gradient
658 Analysis." *Ecology* 80 (7): 2237–53. [https://doi.org/10.1890/0012-
659 9658\(1999\)080\[2237:PCANTF\]2.0.CO;2](https://doi.org/10.1890/0012-9658(1999)080[2237:PCANTF]2.0.CO;2).
- 660 Dormann, Carsten F., Jana M. McPherson, Miguel B. Araújo, Roger Bivand, Janine Bolliger,
661 Gudrun Carl, Richard G. Davies, et al. 2007. "Methods to Account for Spatial Autocorrelation
662 in the Analysis of Species Distributional Data: A Review." *Ecography* 30 (5): 609–28.
663 <https://doi.org/10.1111/j.2007.0906-7590.05171.x>.
- 664 Eason, Tarsha, and Heriberto Cabezas. 2012. "Evaluating the Sustainability of a Regional
665 System Using Fisher Information in the San Luis Basin, Colorado." *Journal of Environmental
666 Management* 94 (1): 41–49. <https://doi.org/10.1016/j.jenvman.2011.08.003>.
- 667 Eason, Tarsha, Ahjond S. Garmestani, Craig A. Stow, Carmen Rojo, Miguel Alvarez-Cobelas,
668 and Heriberto Cabezas. 2016. "Managing for Resilience: An Information Theory-Based
669 Approach to Assessing Ecosystems." *Journal of Applied Ecology* 53 (3): 656–65.
670 <https://doi.org/10.1111/1365-2664.12597>.
- 671 Evans, M. N., S. E. Tolwinski-Ward, D. M. Thompson, and K. J. Anchukaitis. 2013.
672 "Applications of Proxy System Modeling in High Resolution Paleoclimatology." *Quaternary
673 Science Reviews* 76 (September): 16–28. <https://doi.org/10.1016/j.quascirev.2013.05.024>.
- 674 Fisher, R. A. 1922. "On the Mathematical Foundations of Theoretical Statistics."
675 *Philosophical Transactions of the Royal Society of London. Series A, Containing Papers of a
676 Mathematical or Physical Character* 222: 309–68.
- 677 Goring, Simon, Terri Lacourse, Marlow G. Pellatt, and Rolf W. Mathewes. 2013. "Pollen
678 Assemblage Richness Does Not Reflect Regional Plant Species Richness: A Cautionary Tale."
679 Edited by Amy Austin. *Journal of Ecology* 101 (5): 1137–45. [https://doi.org/10.1111/1365-
680 2745.12135](https://doi.org/10.1111/1365-2745.12135).
- 681 Hastie, Trevor, and Werner Stuetzle. 1989. "Principal Curves." *Journal of the American
682 Statistical Association* 84 (406): 502–16.
683 <https://doi.org/10.1080/01621459.1989.10478797>.
- 684 Jackson, Stephen T. 2007. "Looking Forward from the Past: History, Ecology, and
685 Conservation." *Frontiers in Ecology and the Environment* 5 (9): 455–55.
686 [https://doi.org/10.1890/1540-9295\(2007\)5\[455:LFFTPH\]2.0.CO;2](https://doi.org/10.1890/1540-9295(2007)5[455:LFFTPH]2.0.CO;2).
- 687 Karunanithi, Arunprakash T., Heriberto Cabezas, B. Roy Frieden, and Christopher W.
688 Pawlowski. 2008. "Detection and Assessment of Ecosystem Regime Shifts from Fisher
689 Information." *Ecology and Society* 13 (1).
- 690 Killick, Rebecca, and Idris A. Eckley. 2014. "Changepoint: An r Package for Changepoint
691 Analysis." *Journal of Statistical Software* 58 (1): 1–19.
692 <https://doi.org/10.18637/jss.v058.i03>.
- 693 Kim, Dae-Won, Pavlos Protopapas, Yong-Ik Byun, Charles Alcock, Roni Khardon, and
694 Markos Trichas. 2011. "Quasi-Stellar Object Selection Algorithm Using Time Variability and

695 Machine Learning: Selection of 1620 Quasi-Stellar Object Candidates from Macho Large
696 Magellanic Cloud Database." *The Astrophysical Journal* 735 (2): 68.
697 <https://doi.org/10.1088/0004-637X/735/2/68>.

698 Kosnik, Matthew A., and Michał Kowalewski. 2016. "Understanding Modern Extinctions in
699 Marine Ecosystems: The Role of Palaeoecological Data." *Biology Letters* 12 (4).
700 <https://doi.org/10.1098/rsbl.2015.0951>.

701 Liu, Yao, Simon Brewer, Robert K. Booth, Thomas A. Minckley, and Stephen T. Jackson.
702 2012. "Temporal Density of Pollen Sampling Affects Age Determination of the Mid-
703 Holocene Hemlock (*Tsuga*) Decline." *Quaternary Science Reviews* 45 (June): 54–59.
704 <https://doi.org/10.1016/j.quascirev.2012.05.001>.

705 Mann, Michael E., and Scott Rutherford. 2002. "Climate Reconstruction Using
706 'Pseudoproxies'." *Geophysical Research Letters* 29 (10): 139-1-139-4.
707 <https://doi.org/10.1029/2001GL014554>.

708 Mayer, Audrey L., Christopher W. Pawlowski, and Heriberto Cabezas. 2006. "Fisher
709 Information and Dynamic Regime Changes in Ecological Systems." *Ecological Modelling*,
710 Selected Papers from the Third Conference of the International Society for Ecological
711 Informatics (ISEI), August 26–30, 2002, Grottaferrata, Rome, Italy, 195 (1): 72–82.
712 <https://doi.org/10.1016/j.ecolmodel.2005.11.011>.

713 Nun, Isadora, Pavlos Protopapas, Brandon Sim, Ming Zhu, Rahul Dave, Nicolas Castro, and
714 Karim Pichara. 2015. "FATS: Feature Analysis for Time Series." *arXiv:1506.00010*, August.
715 <https://arxiv.org/abs/1506.00010>.

716 Parnell, A. C., J. Haslett, J. R. M. Allen, C. E. Buck, and B. Huntley. 2008. "A Flexible Approach
717 to Assessing Synchronicity of Past Events Using Bayesian Reconstructions of Sedimentation
718 History." *Quaternary Science Reviews* 27 (19): 1872–85.
719 <https://doi.org/10.1016/j.quascirev.2008.07.009>.

720 Payne, Richard, and Maria Gehrels. 2010. "The Formation of Tephra Layers in Peatlands: An
721 Experimental Approach." *CATENA* 81 (1): 12–23.
722 <https://doi.org/10.1016/j.catena.2009.12.001>.

723 Peck, Steven L. 2004. "Simulation as Experiment: A Philosophical Reassessment for
724 Biological Modeling." *Trends in Ecology & Evolution* 19 (10): 530–34.
725 <https://doi.org/10.1016/j.tree.2004.07.019>.

726 Plumpton, Heather, Bronwen Whitney, and Francis Mayle. 2019. "Ecosystem Turnover in
727 Palaeoecological Records: The Sensitivity of Pollen and Phytolith Proxies to Detecting
728 Vegetation Change in Southwestern Amazonia." *The Holocene* 29 (1): 1720–30.
729 <https://doi.org/10.1177/0959683619862021>.

730 R Core Team. 2020. "R: A Language and Environment for Statistical Computing." Vienna,
731 Austria.

- 732 Reitalu, Triin, Pille Gerhold, Anneli Poska, Meelis Pärtel, Vivika Väli, and Siim Veski. 2015.
733 “Novel Insights into Post-Glacial Vegetation Change: Functional and Phylogenetic Diversity
734 in Pollen Records.” Edited by Otto Wildi. *Journal of Vegetation Science* 26 (5): 911–22.
735 <https://doi.org/10.1111/jvs.12300>.
- 736 Richards, Joseph W., Dan L. Starr, Nathaniel R. Butler, Joshua S. Bloom, John M. Brewer,
737 Arien Crellin-Quick, Justin Higgins, Rachel Kennedy, and Maxime Rischard. 2011. “On
738 Machine-Learned Classification of Variable Stars with Sparse and Noisy Time-Series Data.”
739 *The Astrophysical Journal* 733 (1): 10. <https://doi.org/10.1088/0004-637X/733/1/10>.
- 740 Roberts, Caleb P., Dirac Twidwell, Jessica L. Burnett, Victoria M. Donovan, Carissa L.
741 Wonkka, Christine L. Bielski, Ahjond S. Garmestani, et al. 2018. “Early Warnings for State
742 Transitions.” *Rangeland Ecology & Management* 71 (6): 659–70.
743 <https://doi.org/10.1016/j.rama.2018.04.012>.
- 744 Simpson, G. L., and J. Oksanen. 2020. *Analogue Matching and Modern Analogue Technique*
745 *Transfer Function Models. Version 0.17-4*.
- 746 Simpson, Gavin L., and H. John B. Birks. 2012. “Statistical Learning in Palaeolimnology.” In
747 *Tracking Environmental Change Using Lake Sediments: Data Handling and Numerical*
748 *Techniques*, edited by H. John B. Birks, André F. Lotter, Steve Juggins, and John P. Smol, 249–
749 327. Developments in Paleoenvironmental Research. Dordrecht: Springer Netherlands.
750 https://doi.org/10.1007/978-94-007-2745-8_9.
- 751 Smerdon, Jason E. 2012. “Climate Models as a Test Bed for Climate Reconstruction
752 Methods: Pseudoproxy Experiments.” *WIREs Climate Change* 3 (1): 63–77.
753 <https://doi.org/10.1002/wcc.149>.
- 754 Sokolovsky, K. V., P. Gavras, A. Karampelas, S. V. Antipin, I. Bellas-Velidis, P. Benni, A. Z.
755 Bonanos, et al. 2017. “Comparative Performance of Selected Variability Detection
756 Techniques in Photometric Time Series.” *Monthly Notices of the Royal Astronomical Society*
757 464 (1): 274–92. <https://doi.org/10.1093/mnras/stw2262>.
- 758 Spanbauer, Trisha L., Craig R. Allen, David G. Angeler, Tarsha Eason, Sherilyn C. Fritz,
759 Ahjond S. Garmestani, Kirsty L. Nash, and Jeffery R. Stone. 2014. “Prolonged Instability
760 Prior to a Regime Shift.” Edited by John A. D. Aston. *PLoS ONE* 9 (10).
761 <https://doi.org/10.1371/journal.pone.0108936>.
- 762 Spanbauer, Trisha L., Craig R. Allen, David G. Angeler, Tarsha Eason, Sherilyn C. Fritz,
763 Ahjond S. Garmestani, Kirsty L. Nash, Jeffery R. Stone, Craig A. Stow, and Shana M.
764 Sundstrom. 2016. “Body Size Distributions Signal a Regime Shift in a Lake Ecosystem.”
765 *Proceedings of the Royal Society B: Biological Sciences* 283 (1833).
766 <https://doi.org/10.1098/rspb.2016.0249>.
- 767 Taranu, Zofia E., Stephen R. Carpenter, Victor Frossard, Jean-Philippe Jenny, Zoë Thomas,
768 Jesse C. Vermaire, and Marie-Elodie Perga. 2018. “Can We Detect Ecosystem Critical
769 Transitions and Signals of Changing Resilience from Paleo-Ecological Records?” *Ecosphere*
770 9 (10). <https://doi.org/10.1002/ecs2.2438>.

- 771 Telford, R.J., Heegaard, E., Birks, H.J.B., 2004. All Age-Depth Models Are Wrong: But How
772 Badly? *Quaternary Science Reviews* 23, 1–5.
773 <https://doi.org/10.1016/J.QUASCIREV.2003.11.003>
- 774 Williams, John W., Jessica L. Blois, and Bryan N. Shuman. 2011. “Extrinsic and Intrinsic
775 Forcing of Abrupt Ecological Change: Case Studies from the Late Quaternary.” *Journal of*
776 *Ecology* 99 (3): 664–77. <https://doi.org/10.1111/j.1365-2745.2011.01810.x>.
- 777 Wilmshurst, Janet M., Matt S. McGlone, and Dan J. Charman. “Holocene Vegetation and
778 Climate Change in Southern New Zealand: Linkages between Forest Composition and
779 Quantitative Surface Moisture Reconstructions from an Ombrogenous Bog.” *Journal of*
780 *Quaternary Science* 17, no. 7 (2002): 653–66. <https://doi.org/10.1002/jqs.689>.
- 781 Zurell, Damaris, Uta Berger, Juliano S. Cabral, Florian Jeltsch, Christine N. Meynard, Tamara
782 Münkemüller, Nana Nehrbass, et al. 2010. “The Virtual Ecologist Approach: Simulating Data
783 and Observers.” *Oikos* 119 (4): 622–35. [https://doi.org/10.1111/j.1600-](https://doi.org/10.1111/j.1600-0706.2009.18284.x)
784 [0706.2009.18284.x](https://doi.org/10.1111/j.1600-0706.2009.18284.x).